



Effect of Side Groove Shapes on Shear Lips Formation of Aluminium Alloy 6061 using Finite Element Analysis

Muhammad Al-Fayyidh Mohd Al-Hatta¹, Mohd Azhar Harimon^{1*}

¹Faculty of Mechanical and Manufacturing Engineering,
Universiti Tun Hussien Onn Malaysia, Parit Raja, Batu Pahat, 86400, MALAYSIA

*Corresponding Author

DOI: <https://doi.org/10.30880/jamea.2022.03.02.004>

Received 24 July 2022; Accepted 23 August 2022; Available online 13 December 2022

Abstract: Aluminium alloy 6061 is known for its superior mechanical characteristics, which include lighter weight properties, high specific strength, and simple fabrication. Hence, they are widely used to reduce the weight of vehicles as structural parts. Aluminium alloy 6061 is subjected to high velocity and various forces in the course of an accident. Hence, understanding the impact properties of aluminium alloys is critical. The impact of side groove shapes on the shear lip development of aluminium alloy 6061 was examined in this work. The shapes of the side groove in this study are V-shape, U-shape, and square-shape. By simulation using Abaqus software, the Charpy impact test was conducted to determine the shear lips ratio, energy absorbed, displacement and force. It was found that the V-shape side groove shape has the lowest absorb energy as compared to the U-shape and square-shape. The low absorbed energy indicates that the behaviour of the sample test is in a fast-moving brittle fracture. Furthermore, it can be observed that the shear lips for V-shape and square-shape have the lowest ratio of shear lips compared to the U-shape of the side groove. The lower a material's shear lips ratio, the more likely it is to become brittle. In conclusion, when the shear lips ratio is low, it will tend to be low ductility of aluminium alloy 6061, the energy absorbed is low, and the impact of the force is also low.

Keywords: Charpy impact test, side groove shapes, shear lips ratio, aluminium alloy 6061, FEM simulation

1. Introduction

Aluminium alloy 6061 is a standard grade aluminium alloy that comes in various shapes and sizes and can be utilised in various applications. 6061 aluminium tooling plate, 6061 aluminium plate and 6061 aluminium extrusions or bars are all examples of this. It is frequently the alloy of choice for applications including furniture, yachts, and general engineering. The reason is that it can blend with different alloying metals to acquire wanted qualities and may be made in a variety of methods. Aluminium alloy 6061 is broadly utilised in the field of engineering. For example, to build structures and various engineering designs [1]. Aluminium alloy 6061, also known as Al6061 is generally utilised in the construction industry, and body pieces, suspension parts, and power-train castings are examples of automobile components [2]. Each of the materials that go through the fracture process has its behaviour of fracture. Fracture behaviour is commonly associated with micro-mechanics fractures and, in terms of stability, the fracture process. The fracture characteristic of a material is labelled as either brittle or ductile [3]. Due to its behaviour, pure Aluminium often cracks in a ductile way [4].

Plastic deformation on the crack tip of the fractured body varies in its dimensions and is commonly referred to as the formation of a shear lip. The shear lip creation is crucial to understanding this fracture behaviour. Slant fracture is reflected by a plastic region or shear lip generated on the surface of the fracture at the specimen's side. According to a previous study, the shear lip small region with even not more than 10% is equal to brittle fracture and quick crack propagation [5]. Furthermore, the shear lips ratio is also influenced by loading rates and specimen thickness. According

to certain studies, adding a side groove to a notch or cracked front can increase the fraction of the notch or cracked front that displays plane strain characteristics [6]. The fractured condition of an aluminium alloy is crucial for determining its ductility and the extent of the plastic distortion or shear lip. Furthermore, brittle fracture is defined as minor or no plastic distortion near the fracture tip [7].

Simulation can be done in any relevant software, one of them is Abaqus software. It may also be used to execute the Charpy impact test. It must be done correctly to produce the same results as the experiment. The test model's three essential components are the striker, anvils, and specimen [8]. The mesh may separate into two types which are coarse mesh and fine mesh in the notch region in the remainder of the specimen [8]. Furthermore, shear lip development during a fracture would be estimated using Abaqus software. According to studies, shear damage is greatest in a slant plane, resulting in shear lip development. The Abaqus programme can calculate the fracture energy and the maximum Von Mises stress, maximum displacement, and absorbed energy by impact [9].

Numerous research has examined how side grooves affect deformation conditions for grooved side samples as well as fracture behaviour, crack initiation, stress, and strain [10-12]. Nevertheless, the impact of different side-groove shapes received just small attention in published studies in this area. The side groove specimen test methodology is a significant and appropriate test method, especially when high loading rates are involved. Therefore, more study on the influence of side groove shapes on the fracture behaviour of the aluminium alloy is critical. In this work, the FEM of the Charpy impact test will be used in conjunction with the FEA software, which is Abaqus, to analyse the fracture behaviour of aluminium alloy 6061.

2. Materials and Methods

2.1 The Parameter and The Material Used for The Specimen

In this study, aluminium alloy 6061 (Al6061) is used to make the specimen model, whereas stainless steel is used to make the striker model. According to ASTM E23's requirements, the chosen material is stainless steel [13]. The material characteristics of stainless steel and Al6061 are displayed in Table 1. The Abaqus software was used to simulate the Charpy impact test, with the striker model's beginning velocity set to 2500 mm/s. Fig. 1 depicts the model developed for the Charpy impact test. The model was designed in a rectangular shape with a V-notch. The specimen's dimensions were fixed at 55 mm x 10 mm x 10 mm for length, width, and depth, respectively. The samples were fabricated following ASTM A370. The V-notch height applied to the model was set to 2 mm, the length to 1.66 mm, and the angle to 45°. Next, the radius of the striker model was fixed to 0.8 mm at one end and 20 mm across its length, with a 1.5 mm gap between the specimen and the striker model. The model's centre, where it was placed over the notch, was where the side groove was carved. On the specimen model, the side groove was depicted as having various side groove shapes with a fix of side groove depth of 1 mm. Moreover, the front and back of the model also had a double side groove. To examine the formation of shear lips, energy absorption, and force needed for each various side groove shape. Different side groove shapes are V-shaped, U-shaped, and Square-shaped. This part should include a description of the specifications and attributes of the tools, supplies, and other resources used in the current investigation.

Table 1 - Al6061 and stainless-steel material properties

Parameter	Specimen Model	Striker Model	Unit or Dimension
Young's Modulus, E	70.0	193.0	GPa
Poisson's Ratio, ν	0.33	0.31	-
Density, ρ	2600	7750	kg/m ³

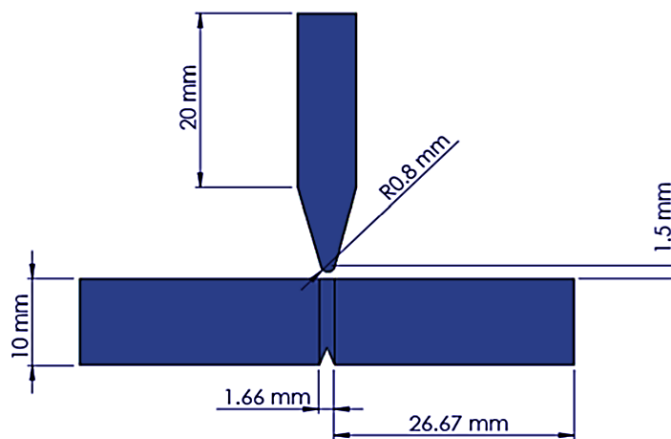


Fig. 1 - The Charpy impact test full assembly with their dimensions

2.2 Process Flow for Finite Element Modelling

The process flow must be well understood by conducting a simulation test using the software. Every action must be taken with caution. If not, it will affect the outcome in the end. Fig. 2 depicts the process flow that was employed in this study. Because of its ability to predict failures in a wide range of engineering materials, for this project, the Johnson-Cook model was applied to describe fracture in Al6061 [14]. For the specimen model, the Johnson-Cook material model was employed in line with the parameter for Al6061 acquired from the other study experiment, as shown in Tables 2 and 3 [15].

Fig. 3 depicts the surface-to-surface contact connection made between the specimen and striker model. It has two main surfaces that can gather information on absorbing force and energy and analyse fracture behaviour. Fig. 4 depicts the Charpy impact test meshing. Since meshing represented an element, it was necessary, and the meshing criterion affected how long it took to solve a problem. In one study, a sweep technique was used to make a hexagonal shape that was then applied with a notch to the centre of a specimen model. Other investigations, on the other hand, employed a structured approach to make a hexagonal mesh shape.

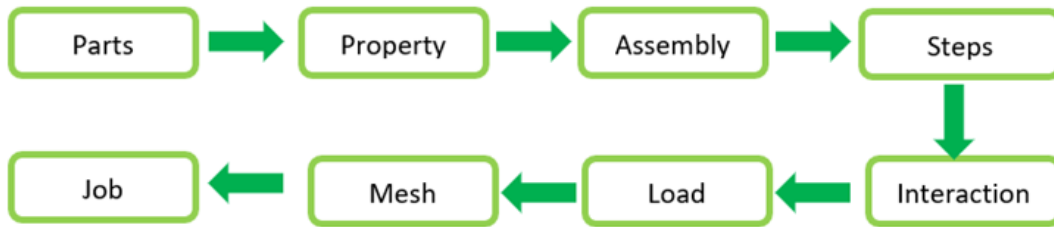


Fig. 2 - The full flow of the process for the simulation by using Abaqus software

Table 2 - Aluminium alloy 6061 Johnson-Cook material model [15]

Parameter	Value	Unit or Dimension
A	324	MPa
B	114	MPa
n	0.42	-
m	1.34	-
c	0.002	-

Table 3 - Johnson-Cook aluminium alloy 6061 damage model [15]

Parameter	Value
d1	0.77
d2	1.45
d3	0.47
d4	0
d5	1.6

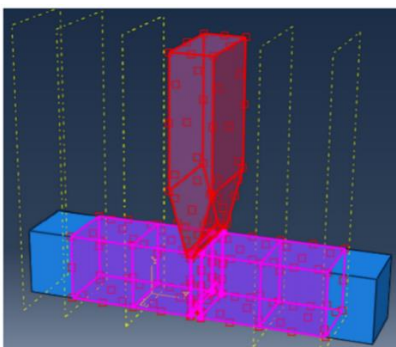


Fig. 3 - The specimen model's and striker model's surface-to-surface contact

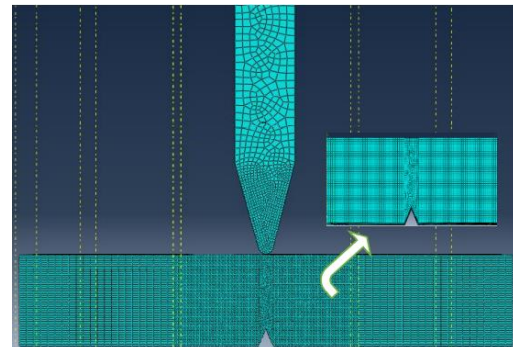


Fig. 4 - The Charpy impact test model has fully meshed

3. Results and Discussion

Based on some studies, the PEEQ technique, which in Abaqus means for plastic strain contours, is demonstrated for each instance of side groove at the crack's cross-sectional face to calculate and estimate the shear lip ratio [16]. This shear lip ratio is then used to see if the grooves are prone to ductile or brittle fractures. The specimen will experience and act as brittle material if the shear lip ratio is less than 10% [17]. In addition, according to the side groove shapes, Fig. 5 shows the fracture surface with shear lips. The ASTM E23 table was used to compute the shear lips ratio, and the graph in Fig. 6 shows the shear lips ratio value in this study. Shear lip growth is characterised by a facial crack with a green colour on both sides. Shear lips ratios greater than 10% were reported in all side groove shapes. This demonstrates that ductile fracture, as opposed to brittle fracture, occurred in all the specimens. As seen in Fig. 6, the shear lips ratio for the V-shaped side groove is the lowest. Shear lips ratio declines, making ductile fractures more brittle. This is because the brittle fracture was more likely to occur the smaller the shear lips ratio.

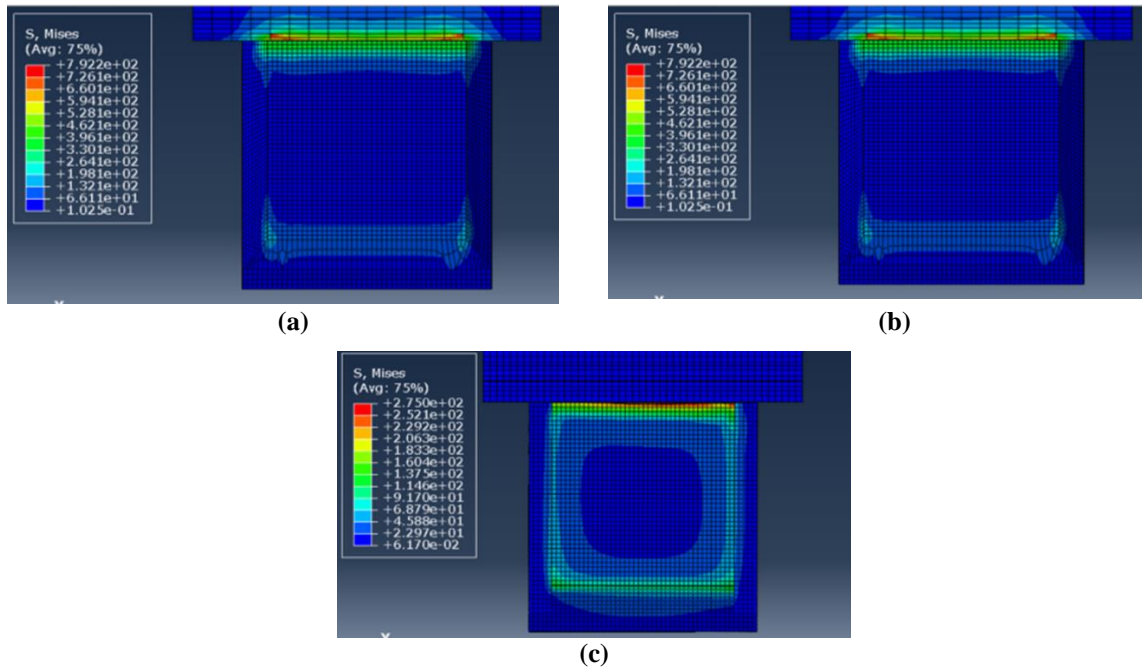


Fig. 5 - Specimen surface that contains the formation of the shear lip for various shape grooves, (a) V-shaped; (b) Square-shape; (c) U-shaped

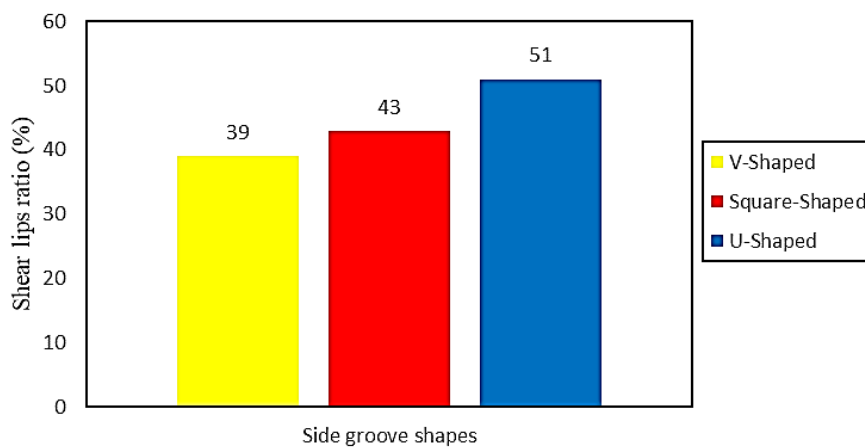


Fig. 6 - Relationship of side groove shapes toward the shear lips formation ratio

Table 4 compares the study's estimations for the shear lips ratio, maximum absorption energy, maximum displacement, and maximum force for various side groove forms. For maximum absorption energy, data was collected using Abaqus features via ODB history output. Absorption energy played a significant role in the Charpy impact test. Following the completion of the time increment up to 0.002 seconds, the data were gathered. According to the graph in Fig. 7, the maximum absorption energy for the V-shape side groove is the lowest, demonstrating that as absorption energy

drops, the specimen would display brittle fracture behaviour. The data's pattern aligns with earlier research's conclusions [18]. Fig. 8 depicts the total absorption energy related to the time increment for each scenario. When compared to other experimental research, the results show that different side groove shapes display distinct brittle behaviour. When the Charpy impact test was performed, the specimen with the lowest shear lips development resulted in the lowest absorption energy. As a result, the lower absorption energy during fracture will result in rapid crack propagation or brittle fracture.

Table 4 - The fracture characteristics of Al6061 at various side groove shapes

Side Groove Shapes	Shear Lips Ratio (%)	Maximum Absorb Energy (J)	Maximum displacement (mm)	Maximum Force (N)
V-Shaped	39	677.994	3.53825	2388.51
Square-Shaped	43	1581.49	3.36876	3200.17
U-Shaped	51	1719.66	3.18830	3355.493

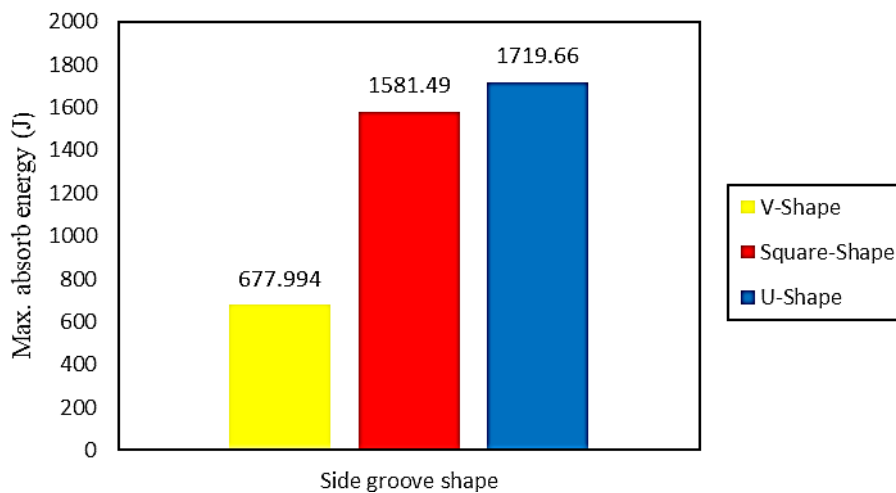


Fig. 7 - The bar chart represents the maximum energy absorbed against the different types of side groove shapes

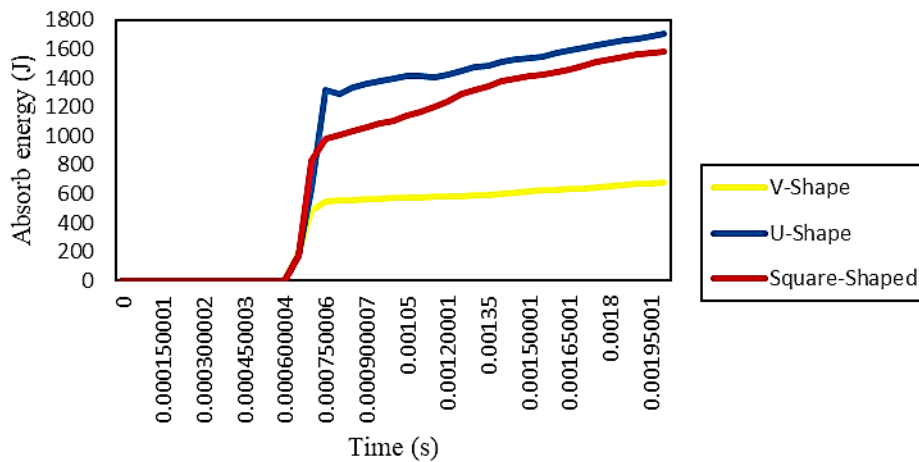


Fig. 8 - Absorb energy versus time graph of aluminium alloy 6061 with various side groove shapes

Fig. 9 then shows the fracture displacement data for the specimen model for numerous side groove shapes. The outcome, which took 0.002 seconds to complete, demonstrated how much damage was done to the specimen model by the crack or fracture. Furthermore, the displacement axis is altered numerous times to attain the maximum value, and the first half of Fig. 9 may be viewed as a parallel line to the time axis. This parallel line represents the incubation period. This suggests that the Al6061 does not fracture during this time but begins to crack following the incubation period [19].

The displacement versus time charts reveal that the V-shaped side groove has a higher displacement. The most displacement is found in the V-shaped side groove. It tends to fracture easier because it has sharp edges V-shaped.

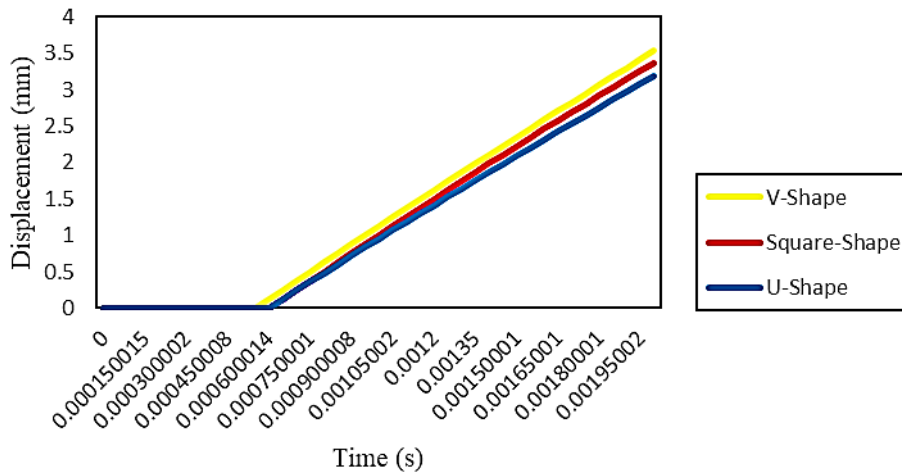


Fig. 9 - The displacement versus time graph for various side groove shapes

For Charpy impact test experiment testing, force is one thing that is important to discuss the maximum force needed to fracture the specimen with the presence of side grooves in different shapes. Based on the graph that has been plotted in Fig. 10 shows the value for the maximum force for each side groove shape. A set of forces data in Fig. 10 represented the Impact Force after 0.002 seconds of incrementation time. The maximum forces indicate the required forces for the specimen model to fracture into two pieces. It can be observed that the trend for the graph is when at a certain displacement, it reaches a higher value of force. After that, the force will decrease because the specimen starts to fracture into two pieces. J. Fang et al. research shows that the maximum force obtained can be defined as the crack initiation nominal start [20]. The trend of the graph supports the findings of Fang et al., who show that force-displacement behaviour terminates when shear lips form. In addition, the total work done during the collision can be expressed from the graph between force against displacement by calculating the area under the graph. Besides, the fewer maximum forces for each side groove shape, the more brittle the specimen model will be and the easier the specimen to fracture and break into two pieces.

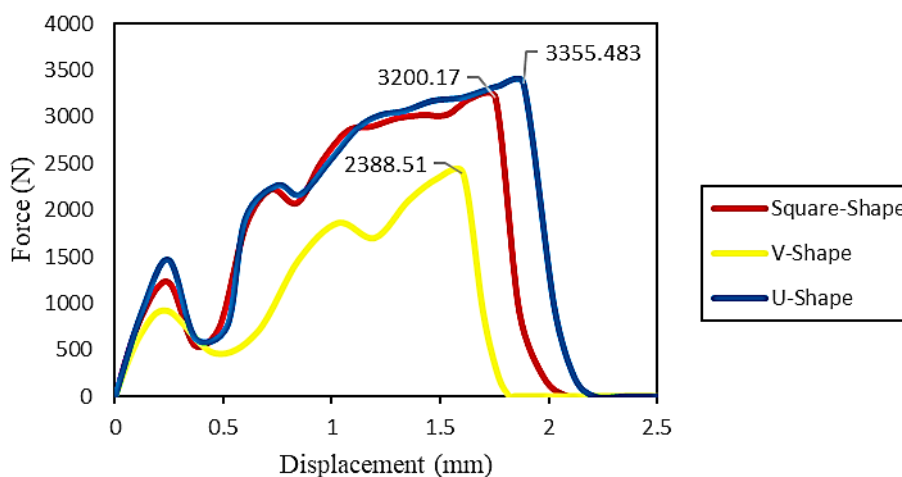


Fig. 10 - The force versus displacement graph for each of the side groove forms

4. Conclusion

A Charpy impact test was performed using the finite element method (FEM) in Abaqus software for aluminium alloy 6061 applications under a range of side groove forms. Plastic strain contours demonstrated a reduction in shear lips for side groove forms such as V, square, and U. As can be seen, the shear lips ratio is greater than 10%. The smallest value is 39%, which indicates the shear lips ratio for V-shape. This may be expected since the Al6061 is still ductile and will undergo plastic deformation before it is broken. Less absorb energy is required on the specimen model when the V-

shaped side groove is employed, as less absorb energy leads to brittle fracture. Furthermore, when the energy absorbed is minimal, as, in the V-shaped side groove, the force required to fracture the specimen is reduced. It takes less force to shatter the specimen model until it is entirely fractured. To summarise, it can be concluded that the data obtained throughout the test in simulation in Abaqus software is relevant compared to research to validate this study as the V-shape side groove has the highest brittle fracture, low absorb energy and a low force of impact.

Acknowledgment

The authors would also like to thank the Faculty of Mechanical and Engineering, University Tun Hussein Onn Malaysia for its support.

References

- [1] J. C. Benedyk, "Aluminum alloys for lightweight automotive structures," in *Materials, design and manufacturing for lightweight vehicles*, Elsevier, 2010, pp. 79-113.
- [2] M. A. Asry and M. A. Harimon, "Effect of Side Groove on Shear Lips Formation of Aluminium Alloy 6061 using Finite Element Analysis," *J. Adv. Mech. Eng. Appl.*, vol. 2, no. 1, pp. 41-48, 2021.
- [3] X. K. Zhu and J. A. Joyce, "Review of fracture toughness (G, K, J, CTOD, CTOA) testing and standardisation," *Eng. Fract. Mech.*, vol. 85, pp. 1-46, 2012.
- [4] H. R. Kotadia, G. Gibbons, A. Das, and P. D. Howes, "A review of Laser Powder Bed Fusion Additive Manufacturing of aluminium alloys: Microstructure and properties," *Addit. Manuf.*, vol. 46, p. 102155, Oct. 2021.
- [5] M. H. Kadhim, N. A. Latif, M. A. Harimon, A. A. Shamran, and D. R. Abbas, "Effects of side-groove and loading rate on the fracture properties of aluminium alloy AL-6061," *Materwiss. Werksttech.*, vol. 51, no. 6, pp. 758-765, 2020.
- [6] F. Di Gioacchino, E. Lucon, E. B. Mitchell, K. D. Clarke, and D. K. Matlock, "Side-grooved Charpy impact testing: Assessment of splitting and fracture properties of high-toughness plate steels," *Eng. Fract. Mech.*, vol. 252, p. 107842, Jul. 2021.
- [7] A. P. Mouritz, "Fracture processes of aerospace materials," in *Introduction to Aerospace Materials*, Woodhead Publishing Limited, 2012, pp. 428-453.
- [8] Y. Cao, Y. Zhen, M. Song, H. Yi, F. Li, and X. Li, "Determination of Johnson-Cook parameters and evaluation of Charpy impact test performance for X80 pipeline steel," *Int. J. Mech. Sci.*, vol. 179, p. 105627, 2020.
- [9] A. Hosseinzadeh, S. H. Hashemi, H. Rastegari, and M. R. Maraki, "Investigation of the notch depth effect on Charpy fracture energy and fracture surface features of API X65 steel," *Can. Metall. Q.*, pp. 1-13, 2022.
- [10] J. Mao, X. Li, S. Bao, L. Luo, and Z. Ding, "Comparative Study of the Geometric Effects on Fracture Behaviors of Side-Grooved and Plain-Sided Compact Tension Specimens," *J. Mater. Eng. Perform.*, vol. 28, no. 10, pp. 6514-6524, Oct. 2019.
- [11] P. Wang, W. Hao, J. Xie, F. He, F. Wang, and C. Huo, "Stress Triaxial Constraint and Fracture Toughness Properties of X90 Pipeline Steel," *Metals (Basel)*, vol. 12, no. 1, p. 72, Jan. 2022.
- [12] Y. Huang and W. Zhou, "Stress intensity factor for clamped SENT specimen containing non-straight crack front and side grooves," *Theor. Appl. Fract. Mech.*, vol. 93, pp. 116-127, Feb. 2018.
- [13] C. N. McCowan, T. A. Siewert, and D. P. Vigliotti, *Charpy verification program: reports covering 1989-2002*. US Department of Commerce, National Institute of Standards and Technology, 2003.
- [14] A. Banerjee, S. Dhar, S. Acharyya, D. Datta, and N. Nayak, "Determination of Johnson cook material and failure model constants and numerical modelling of Charpy impact test of armour steel," *Mater. Sci. Eng. A*, vol. 640, pp. 200-209, 2015.
- [15] S. Pervaiz, S. Kannan, K. Ram, and W. A. Samad, "Numerical modeling of Charpy impact test to determine the fracture characteristics of aluminium alloy 6061," in *Fracture, Fatigue, Failure and Damage Evolution*, Volume 6, Springer, pp. 85-88, 2019.
- [16] K. Jayakrishna, G. Rajiyalakshmi, and A. Deepa. "Structural health monitoring of fiber polymer composites." In *Structural Health Monitoring of Biocomposites, Fibre-Reinforced Composites and Hybrid Composites*, pp. 75-91. Woodhead Publishing, 2019.
- [17] B. P. Ingale and P. S. M. Jadhav, "Characterisation of Bending behavior of Welded Joint," *Int. J. Sci. Res. Dev.*, vol. 5, no. 05, pp. 2321-0613, 2017.
- [18] *International Alloy Designations and Chemical Composition Limits for Wrought Aluminum and Wrought Aluminum Alloys*. Arlington: The Aluminum Association, 2018.

- [19] D. Madhusudhan, S. Chand, S. Ganesh, and U. Saibhargavi, "Modeling and simulation of Charpy impact test of maraging steel 300 using Abaqus," in *IOP Conference Series: Materials Science and Engineering*, 2018, vol. 330, no. 1, p. 1, 2013.
- [20] J. Fang, J. Zhang, and L. Wang, "Evaluation of cracking behavior and critical CTOA values of pipeline steel from DWTT specimens," *Eng. Fract. Mech.*, vol. 124, pp. 18-29, 2014.